Large Eddy Simulation of Wind Turbine Wakes in Prescribed Neutral and Non-Neutral Atmospheric Boundary Layers

Chivaee, Hamid Sarlak; Sørensen, Jens Nørkær

Published in:
Journal of Physics: Conference Series (Online)

Link to article, DOI:
10.1088/1742-6596/555/1/012087

Publication date:
2014

Document Version
Publisher's PDF, also known as Version of record

Large Eddy Simulation of Wind Turbine Wakes in Prescribed Neutral and Non-Neutral Atmospheric Boundary Layers

2014 J. Phys.: Conf. Ser. 555 012087

(http://iopscience.iop.org/1742-6596/555/1/012087)

Large Eddy Simulation of Wind Turbine Wakes in Prescribed Neutral and Non-Neutral Atmospheric Boundary Layers

Hamid Sarlak Chivaee and Jens N. Sørensen
Department of Wind Energy, Technical University of Denmark, Denmark
E-mail: hsar@dtu.dk

Abstract. Large eddy simulation (LES) of an infinitely long wind farm in a fully developed flow is carried out based on solution of the incompressible Navier-Stokes equations. The wind turbines are modeled as equivalent rotating actuator disks by applying aerodynamic loads on the flow field using tabulated aerodynamic lift and drag coefficients to save computational time. As a substitute to standard wall modeling LES, a "prescribed mean shear" profile (hereafter called PMS) approach has been implemented and analysed for generating the desired turbulent shear flow. It is applied on Neutral, Stable and Convective atmospheric boundary layers in presence of the -actuator disc represented- wind turbines and qualitatively meaningful results of mean and fluctuating velocity field is obtained. The effect of four different sub-grid scale (SGS) models on the flow structure is investigated and it is seen that subgrid scale modeling (in particular, the Mix-O and Smagorinsky models) improves the accuracy of the simulations. An optimal grid resolution is also proposed for this kind of simulation.

1. Introduction

Direct simulation of wind turbines in the atmospheric boundary layer is impossible, at least for the near future, because of the need to resolve both the smallest (known as Kolmogorov scales) and the large flow structures (integral scales), requiring a total combination of grid cells and time steps of $\sim Re^3$ with the Reynolds number, Re, being in the order of 10^9. A detailed discussion can be found in [1] and [2].Even when wall modeling is used in combination with coarser grids, simulation of the atmospheric boundary layer in a complex terrain or a wind farm, usually requires a precursor simulation (usually channel flow) to make a realistic turbulent flow and then a successor simulation which includes the desired geometry such as wind turbines in the complex terrain. This method demands a long simulation time. Several studies of wake effects in the wind farm have been performed using the precursor/successor approach e.g., [5, 6].

As opposed to the mentioned precursor/successor approach, a method has been implemented in this paper in which a desired mean arbitrary boundary layer is preserved throughout the simulation. This boundary layer is enforced through the computational domain using body forces similar to an immersed boundary method. The body forces are then stored and applied on the domain through the simulation and the boundary layer shape will be modified due to the interaction of the turbine wakes and buoyancy contributions. This method has been tested for a neutral case and inlet-outlet boundary conditions and it was observed that the it's capable of

capturing the most important features of wakes of a wind turbine as reported in [4] while having the advantage of performing a fast simulation suitable for wake model developments.

2. Actuator disc model

For the simulation of wind turbine, a rotating actuator disc (AD) model, as shown in figure 1 and described below, is used. (see also [7]) [1]

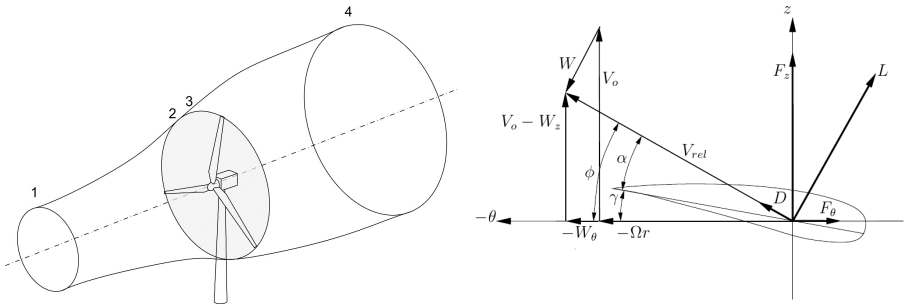

(a) (b)

Figure 1. (a) The AD and it's sorrounding volume (b) Aerodynamics of an airfoil cross section

In the actuator disc model of a turbine of B blades, each rotor is divided to a finite number of sections and for each section, the aerodynamic coefficients are looked up from an accompanying table based on the the relative velocity, angle of attack α and chord length c. The relative velocity on an airfoil element is determined as $V_{rel} = (V_0 + W_z)^2 + (\Omega r + W_\theta)^2$ where V_0 is the free-stream velocity, W_z and W_θ are the induced velocity ($W_z = V_0 - u$ where u is the axial velocity at disc location) and induced angular velocity (defined similarly), respectively, and Ω is the angular velocity of the disc. The flow angle between V_{rel} and the rotor plane is then defined as

$$\phi = tan^{-1}\left(\frac{V_0 - W_z}{\Omega r + W_\theta}\right) \tag{1}$$

The local angle of attack $\alpha = \phi - \gamma$ with γ being the pitch angle should be used for the table look-up to find the C_L and C_D values, according to $(L, D) = 0.5\rho V_{rel}^2 cB(C_L e_L, C_D e_D)$, where e_L and e_D are unit vectors showing the direction of the lift (L) and drag (D) forces. The tangential and normal forces to be exerted on the flow domain are then calculated as

$$F_z = L\ cos(\phi) + D\ sin(\phi) \ \text{ and } F_\theta = L\ sin(\phi) - D\ cos(\phi) \tag{2}$$

The forces are then interpolated from the AD grid to the flow field and applied as body forces using a smoothing function of Gaussian shape.

3. The PMS approach

In order to understand the PMS method, the discretized Navier-Stokes equation on the particular node, P, should be analysed

$$A_p V_p^{t+\Delta t} + \sum_i A_i V_i^{t+\Delta t} = S_p + f_{PMS} \tag{3}$$

[1] In the sub-figure (a), upstream and downstream sections marked with 1-4 are needed for evaluating momentum conservation relations

Table 1. SGS models used for comparisons

Model	**Value**
NO	$\nu_{sgs} = 0$
Smagorinsky	$\nu_{sgs} = cs\Delta^2\|\bar{S}\|$
Mix-S	$\nu_{sgs} = Cm\Delta^{1.5}q_c^{0.25}\|\bar{S}\|^{0.5}$
Mix-O	$\nu_{sgs} = Cm\Delta^{1.5}q_c^{0.25}\|\bar{\Omega}\|^{0.5}$

where the summation is performed over the neighbouring i nodes to P. V is velocity vector, S_p is the body force applied as a source term and $f_{PMS} = f(x, y, x)$ is an external body force which sets a desired velocity field U_d in the computational cell P through the following equation

$$f_{PMS} = A_p U_d^{t+\Delta t} + \sum_i A_i V_i^{t+\Delta t} - S_p \tag{4}$$

4. LES methodology

In LES of the wind farm ABL, the momentum and energy equations i.e.,

$$\begin{aligned} \frac{\partial \tilde{u}_i}{\partial t} + \tilde{u}_j\left(\frac{\partial \tilde{u}_i}{\partial x_j} + \frac{\partial \tilde{u}_j}{\partial x_i}\right) &= -\frac{1}{\rho}\frac{\partial \tilde{p}^*}{\partial x_i} - \frac{\partial \tau_{ij}}{\partial x_j} + \nu\frac{\partial^2 \tilde{u}_i}{\partial x_j^2} \\ &+ \delta_{i3} g\frac{\tilde{\theta} - \langle\tilde{\theta}\rangle}{\theta_0} + f_c\epsilon ij3\tilde{u}_i - \frac{f_i}{\rho} + F_i \qquad (5) \\ \frac{\partial \tilde{\theta}}{\partial t} + \tilde{u}_j\frac{\partial \tilde{\theta}}{\partial x_j} &= -\frac{\partial q_j}{\partial x_j} + \alpha\frac{\partial^2 \tilde{\theta}}{\partial x_j^2} \qquad (6) \end{aligned}$$

are to be solved where $\tilde{\phi}$ represents the filtering operation on the variable ϕ, $\tau_{ij} = \widetilde{u_i u_j} - \tilde{u}_i\tilde{u}_j$ and $q_i = \widetilde{u_j\theta} - \tilde{u_j}\tilde{\theta}$ are the deviatoric part of SGS stress tensor and SGS heat flux respectively, $\tilde{p}^* = \tilde{p} + \rho\tilde{u}_i\tilde{u}_i/2$ is the modified pressure, f_c, f_i, F_i are the Coriolis parameter, wind turbine loading, and external forcing such as wind force. $\tilde{\theta}, \alpha$ are the potential temperature and air thermal diffusivity ($\alpha = \frac{-\nu}{Pr}$ where Pr is the Prandtl number). In this paper, no explicit model is used for the SGS heat flux and only Pr=0.71 is used for the molecular diffusivity approximation.

Four different models are used to evaluate the ν_{sgs} and hence the SGS stress tensor ($\tau_{ij} = -\nu_{sgs}\bar{S_{ij}}$) as shown in table 1. *NO* refers to the case with zero eddy viscosity for which the effects of dissipation are inherent in the the numerical dissipation of the discretization schemes. This choice of an SGS model could result in an accurate solution in cases where the numerical code is dissipative. This is the case in our code, which uses a collocated grid and finite differencing for the derivatives, as opposed to pseudo-spectral codes that reportedly have no numerical dissipation. *Smagorinsky* refers to standard Smagorinsky, and *Mix-S* and *Mix-O* represent two variations of a semi-mixed model originally proposed by (see [10])

with $q_c = (\bar{\tilde{u}_i} - \tilde{u}_i)^2$ being the sub-filter kinetic energy obtained by an explicit filtering (shown by bar) of larger size than the grid size, δ being the grid size, $\Gamma(\tilde{u}(x, y, z, t)) = \tilde{S}_{ij}(x, y, z, t)$ or $\nabla \times \tilde{u}(x, y, z, t)$ (strain rate or vorticity tensor of resolved scales) depending on the nature of the flow and $\alpha \in [0, 1]$. in the current simulations, $\alpha = 0.5$ is used. C_m is the model constant and is chosen to be 0.01 in the current implementation (See also [3]).

5. Simulation results

Simulations are performed usind the CFD code Ellipsys3D (See [9] and [8]), a general purpose multiblock structured parallelized CFD platform. It's based on collocated grid storage

arrangement using Rhie-Chow interpolation for pressure-velocity coupling. It uses an implicit time stepping (CFL number is kept at approximately 0.75) and a blend of fourth order central differencing (90 percent, to be accurate) and third order QUICK (10 percent to smooth wiggles in the flow) scheme for the convective terms in the NS equation and a second order central differencing for the rest of the terms.

For the post-processing, the mean velocities and two components of the turbulent stress tensor are used. Figure 2 shows the simulation domain and some velocity snapshots. Simulations are run for more than 2 hours of real time simulation and time averaging begins after approximately one hour. For comparisons, the streamwise velocity w in both decimal and logarithmic scales (to give a more clear comparison) and the two important components of the turbulent stress tensor, normalized by the bulk velocity and, i.e. $\frac{\overline{<w'w'>}}{U_0^2}$ and $\frac{\overline{<v'w'>}}{U_0^2}$ are chosen, respectively.

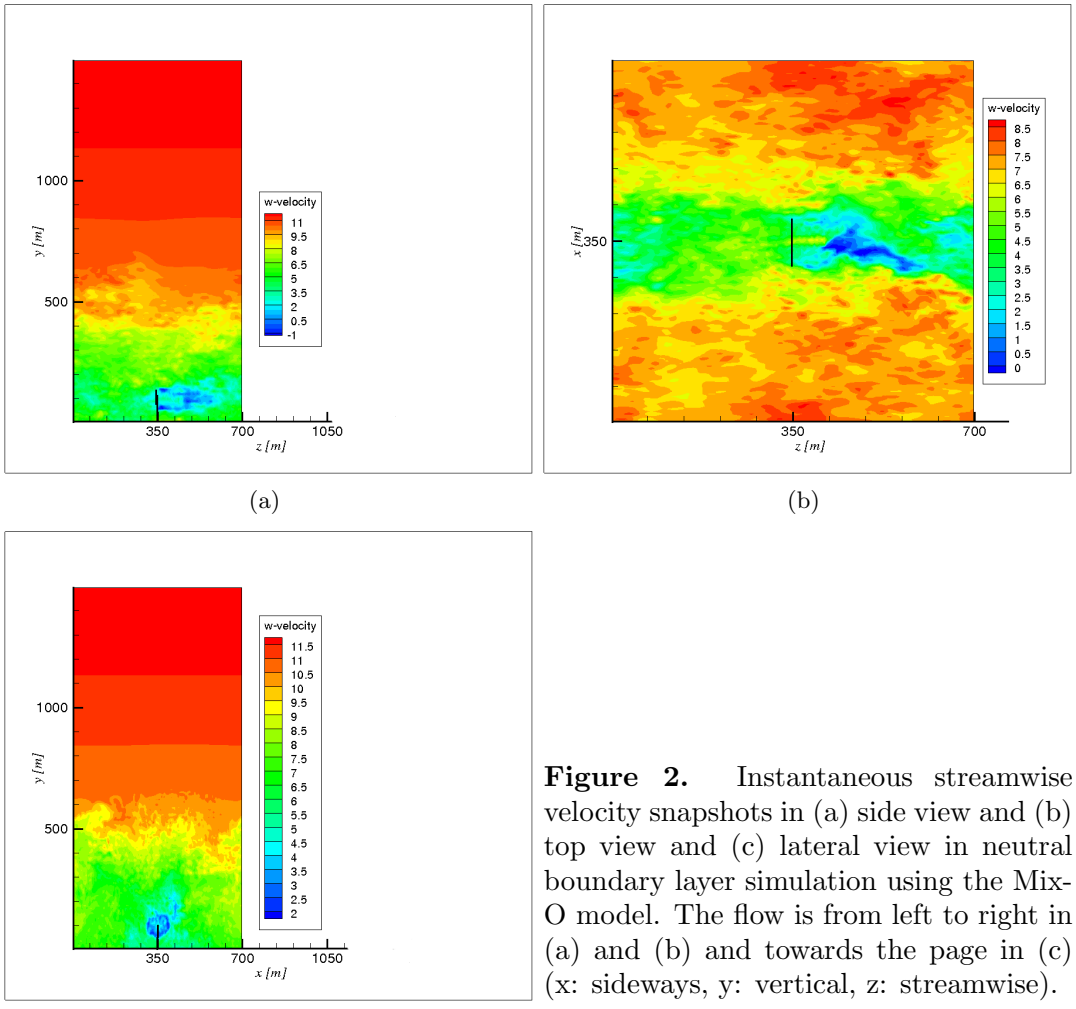

Figure 2. Instantaneous streamwise velocity snapshots in (a) side view and (b) top view and (c) lateral view in neutral boundary layer simulation using the Mix-O model. The flow is from left to right in (a) and (b) and towards the page in (c) (x: sideways, y: vertical, z: streamwise).

All of the simulations start with a prescribed logarithmic velocity profile of $8m/s$ at the hub height. In the simulations, the domain size is set to $700 \times 1500 \times 700m$ in spanwise, vertical and streamwise directions (corresponding velocity components in spanwise x, vertical y and streamwise z coordinates are (u, v, w) respectively). This implies a seven diameter (7D) distance between individual turbines in streamwise and spanwise directions. This choice for the cross-flow dimensions ensures that the blockage factor will be small enough, since $\frac{A_{rot}}{A_d} = 0.008$,

where A_{rot} is the rotor area and A_d is the domain's projected area in streamwise direction (see[11]). The $Tjaereborg$ turbine used has a diameter of $100\,m$ with it's hub located at $(x, y, z) = (350, 100, 350)\,m$, rotating with tip speed ratio of $\lambda = 7.6$ (see [7]). The Reynolds number based on the streamwise bulk flow of $U_0 = 8m/s$ and domain height h is $Re_h = 8 \times 10^8$. Rotor diameter is used to normalize the length scales.

Unlike wall modeling approaches, a slip wall boundary condition is used at the bottom in connection with the use of the PMS; symmetry BC on the top and periodic boundaries on the vertical walls. For the temperature in the stable case (refers to as SBL hereafter), a fixed value of 285 K is applied from the ground up to a height of $1km$, after it which increases linearly with a rate of $3.5K/km$ to take care of the cappping inversion. For the convective (unstable) case (CBL) the temperature is decreased from the wall to a height of 600 m with the same rate as in the SBL case, after which it is fixed at 285 K for the rest of the simulation.

5.1. Grid sensitivity study

The first tests have been performed to evaluate the effect of grid refinement on the simulation results. Three cases of 96^3, 144^3, and 192^3 resolution in neutral ABL condition are compared and the results are presented in figure 3.

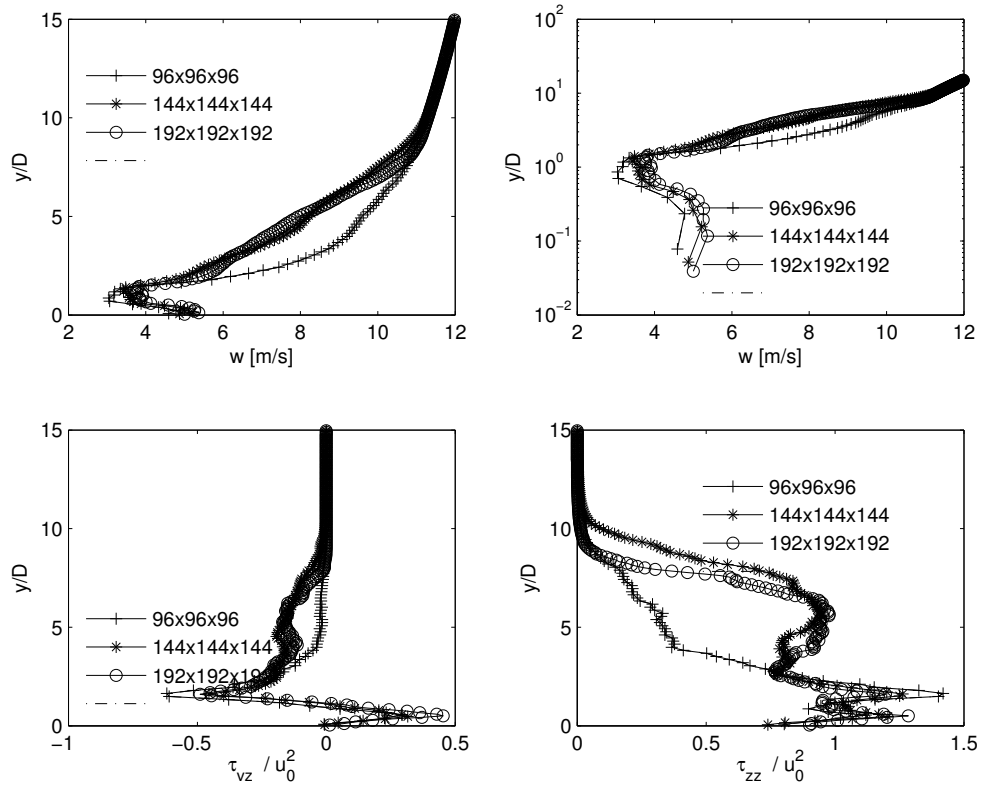

Figure 3. Comparison of (a) mean streamwise velocity, (b) mean streamwise velocity in logarithmic axis, (c) Reynolds shear stress, (d) turbulent normal stress for different grid resolutions. The slice is vertically cut through the rotor plane and the height is normalized by the rotor diameter D. The vertical extent of the rotor is therefore $0.5 \leq y/D \leq 1.5$.

The results suggest that a grid resolution of 144^3 is close to that of the 192^3 cells. This resolution is chosen as a reference hereafter for other comparisons. It is also seen that a coarse resolution, causes a velocity speed-up in a region above the turbine tip and below approximately

10 rotor diameters. This increased velocity contributes to having a lower turbulent mixing in that layer, as observed in the turbulent stress profiles.

5.2. Comparison of the SGS models

In this sections, the neutral ABL case is chosen as a basis to compare the performance of the SGS models. As mentioned earlier, four different models are compared, that is, a no-model LES (Coarse DNS), two mixed models based on the resolved shear strain or vorticity rate, and a standard Smagorinsky model. Figure 4 compares the horizontally averaged streamwise mean velocities as well as the turbulent shear stresses for the different models as a function of domain height. It can be seen that all models are able to predict a true maximum wake deficit at the rotor center. However, the values are quite different close to the wall. Also the NO and Mix-S models give a velocity overshoot which is usually not observed in wind turbine wakes in the neutral ABL (see [5]). All of the models under predict the Reynolds shear stress profile meaning low amount of mixing from the upper surface layer to the turbines. Ideally the shear stress profiles above the turbine will follow the standard $y-1$ line which is also seen in the turbulent channel flows (see also [5]). The turbulent normal stress using the Mix-O and Smagorinsky models are of higher magnitude which is more acceptable. A more detailed comparison of SGS modeling on wind turbine wakes can be found in [12].

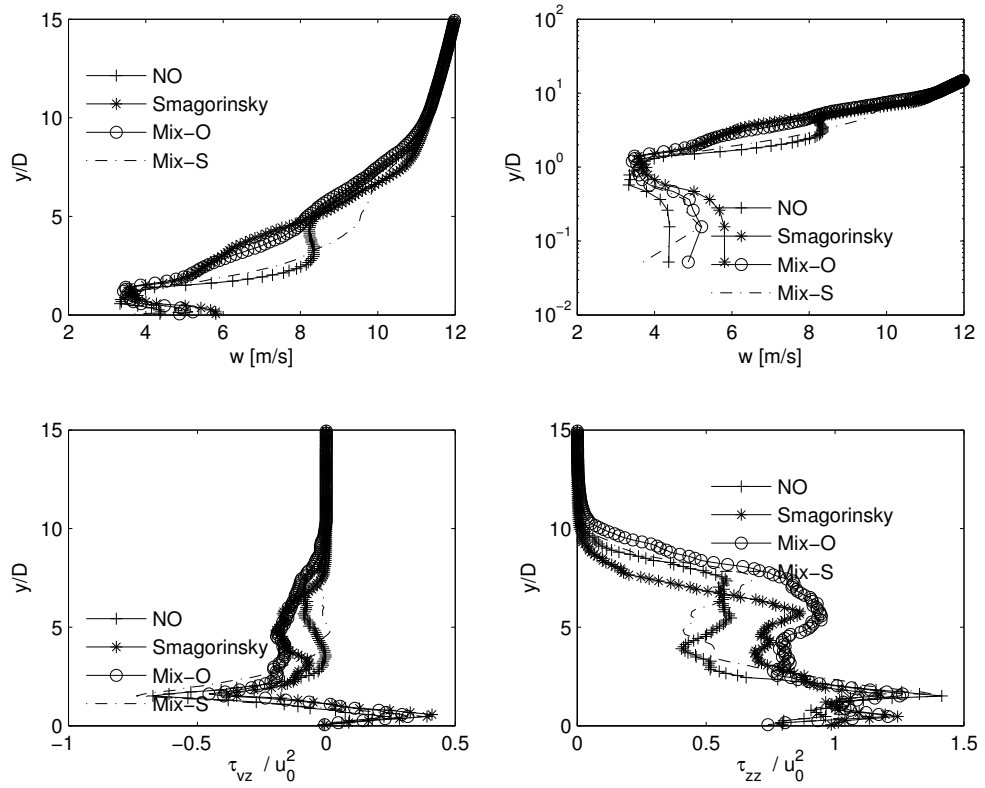

Figure 4. Comparison of different SGS models for the neutral ABL case with grid resolution of 144^3. Same quantities and dimensions as shown in figure 3

5.3. Comparisons of cases with different thermal stabilities

Based on the initial and boundary conditions described above, three cases with neutral (NBL), stable (SBL) and convective (CBL) boundary layers are simulated. The Mix-O model is used for

all cases, as it was shown relatively satisfactory in the previous section. The results are shown in figure 5. It can be seen that there is a notable difference in the horizontally averaged mean velocities. The velocity deficit is highest for the SBL case and lowest for the CBL case. The reason is that in the CBL case, there are large buoyancy forces driving the flow upwards from the ground and cause a strong mixing which in dissipates the flow and results in faster recovery whereas in the SBL case, opposite phenomenon happens and the fluctuations are damped faster, resulting in a longer wake recovery and larger deficits. It can also be seen that for the convective case the mean velocity is smaller throughout the whole domain, which is in agreement with the other studies (see [**?**]). Clearly, the neutral case is somewhere in between CBL and SBL cases. All Reynolds stress components have their peaks at the rotor tips and in agreement with the mean velocity observations, the Reynolds stress is lower for the CBL case showing that the velocity fluctuations are smallest for this case. Fluctuations are of the same magnitude for the NBL and SBL though. The turbulent normal stresses for the stable and neutral case, have their maximum in the wind turbine region and decrease to zero at the top of the domain, where turbulence essentially vanishes. However, the unstable case (CBL) is turbulent over the whole domain, which is again attributed to the large thermal structures driving the flow upwards and enhance the mixing.

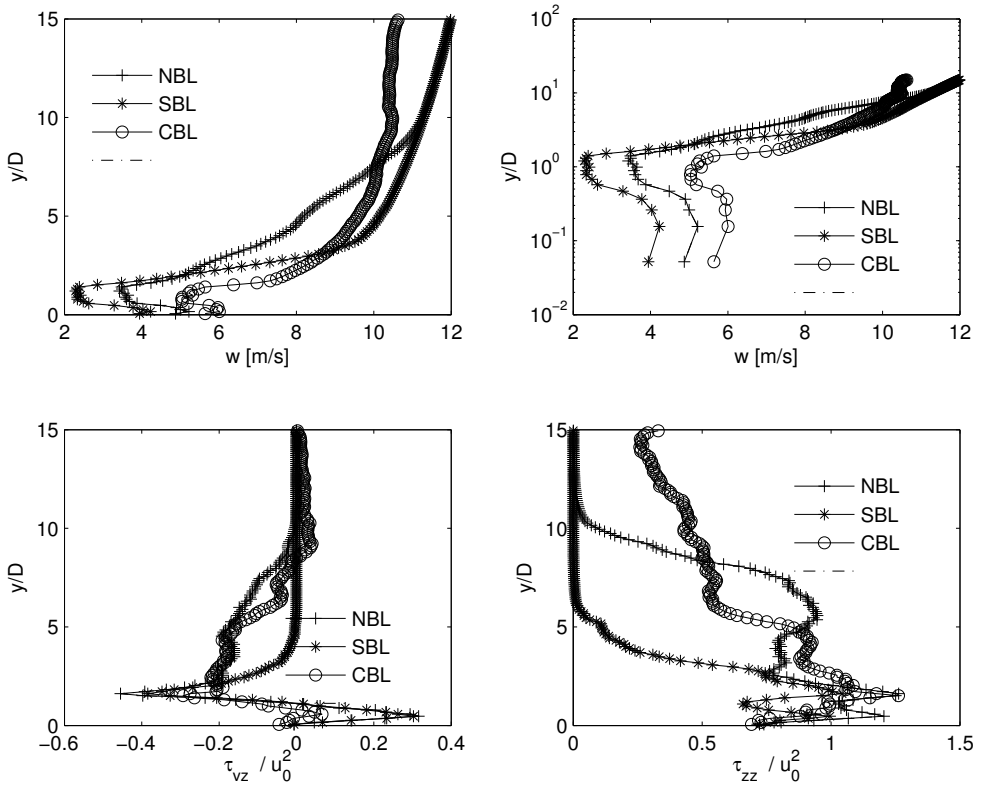

Figure 5. Comparison of neutral (NBL), stable (SBL) and convective (unstable) (CBL) atmospheric boundary layer using the Mix-O model and grid resolution of 144^3. Same quantities and dimensions as shown in figure 3

6. Conclusions

The main aim of this paper was to demonstrate the capability of LES simulations of an infinite wind turbine boundary layer with the PMS method, that is, exerting body forces to maintain

a desired velocity profile and to show that these body forces are generally so smaller than the buoyancy effects and turbine body forces that allow for the turbulent wake structures to develop naturally. The results show that the PMS method gives reasonable estimates of the flow structures at different atmospheric boundary layer regimes, i.e. higher mixing and lower velocity deficit in the CBL case compared to the other cases. Some of the statistics, however, might be questionable especially close to the wall since there is no wall modeling at the bottom. However, besides the significant computational cost improvement, the PMS is very useful in evaluating the wind turbine wake structures in shear flows. The same method can also be applied when any combination of the wind veer (directional variability with height) and Coriolis effects are desired. One should note that this study was only a proof of concept and further validations should be done against available experimental and numerical data in the future. Sensitivity analyses were performed to check the influence of different SGS models and the Smagorinsky and Mix-O models turned out to be more accurate for this kind of study.

6.1. Acknowledgments

The funding for this project was provided through Statkraft Ocean Energy Research Program (SOERP) and the DTU Center for Computational Wind Turbine Aerodynamics and Atmospheric Turbulence (COMWIND). Partial fund from Otto-Mønsted A/S is also gratefully appreciated.

References

[1] Piomelli U 2008 Wall-layer models for large-eddy simulations *Prog Aerosp Sci* **44**, 437-46.
[2] Piomelli U, Benocci C and van Beek J 2012 *Large eddy simulation and related techniques: Theory and applications* Von Karman Institute Lecture Series ISSN0377-8312.
[3] Cavar D 2006 *Large Eddy Simulation of Industrially Relevant Flows*, DTU Denmark.
[4] Troldborg N, Sørensen JN and Mikkelsen RF 2010 Numerical simulations of wake characteristics of a wind turbine in uniform inflow *J Wind Energy* (**13**)1 86-99.
[5] Calaf, M., Meneveau, C., and Meyers, J. 2010 Large eddy simulation study of fully developed wind-turbine array boundary layers. *Physics of Fluids*, **22**(015110).
[6] Lu H., and Porte-Agel, F. 2011 Large-eddy simulation of a very large wind farm in a stable atmospheric boundary layer *Physics of Fluids*, **23**, 065101.
[7] Mikkelsen R, Sørensen JN and Shen WZ 2001 Modelling and Analysis of the Flow Field around a Coned Rotor. *J Wind Energy* **4** 121-35.
[8] Michelsen JA 1992 *Basis3D- A platform for development of multiblock PDE solvers*, Technical report AFM 92-05, Technical University of Denmark.
[9] Sørensen NN 1995 *General purpose flow solver applied to flow over hills*, Risø-R-827-(EN), RisøNational Laboratory, Denmark.
[10] Lenormand E, Comte P, Phuoc, L T, and Sagaut P 2000 Subgrid-Scale Models for Large-Eddy Simulations of Compressible Wall Bounded Flows *AIAA J* **38**(8), 1340–50.
[11] Baetke F and Werner H 1990 Numerical simulation of turbulent flow over surface-mounted obstacles with sharp edges and corners *J Wind Eng Ind Aerod* **(35)** 129-47.
[12] Sarlak H., Meneveau C., Sørensen JN, and Mikkelsen R. 2013 Quantifying the impact of subgrid scale models in actuator-line based LES of wind turbine wakes in laminar and turbulent inflow, Direct and Large-Eddy Simulation IX ERCOFTAC Series, Springer (accepted).